Acta Crystallographica Section A
Foundations of Crystallography
ISSN 0108-7673

Received 28 April 2009
Accepted 6 July 2009

Phase modulation effects in X-ray diffraction from a highly deformed crystal with variable strain gradient

M. Shevchenko

Solid State Theory, Institute for Metal Physics, Vernadsky 36, Kiev 03142, Ukraine. Correspondence e-mail: mishevch@yahoo.com

The X-ray interbranch scattering by lattice distortions is studied for a thin crystal whose thickness is appreciably less than the conventional X-ray extinction length. The concept of interbranch phase modulation of the X-ray wavefield is extended to the case of a large gradient which depends on depth inside the crystal. The prominent interbranch features of the diffracted intensity are also established within this concept. Numerical calculations of the diffracted intensity are presented for an exponential strain gradient model to illustrate this. Diffraction (extinction) contrast is discussed for a strongly deformed specimen containing a single dislocation. It is predicted that for large values of the X-ray extinction length the extinction contrast may arise even in the case of a very thin crystal. This effect, owing to the interbranch phase changes of the waves scattered in the deformed matrix, is observed in experiments with protein crystals.

1. Introduction

X-ray diffraction by highly strained crystals is conventionally treated as a kinematical process (James, 1948). This viewpoint turns out to be correct in many practical cases. However, some X-ray studies on crystals of strongly distorted heterostructures show unexpected results (Tanner & Hill, 1986; Ferrari *et al.*, 2005). Although the actual crystal thicknesses were much less than the extinction lengths involved, it is argued that dynamical diffraction theory should be exploited to explain the observations.

Unfortunately, a comprehensive physical understanding based on Takagi's equations (Takagi, 1969) is difficult to obtain. Normally numerical solutions must be searched. When analytical solutions are obtained, they usually involve special mathematical functions which do not provide an interpretation in terms of a wavefield concept. Bearing this in mind, we present an alternative dynamical approach applicable for the case of a variable strain gradient depending on the depth z inside a crystal. This approach, which takes into account X-ray interbranch scattering, is capable of explaining the dynamical diffraction effects in highly deformed thin crystals. This topic was first considered by Penning (1966) and has been intensively studied by Authier and co-workers (Authier, 2005).

In this work, it is assumed that deformations of lattice exceed the limit of validity of the eikonal theory. This limit, established by Authier & Balibar (1970), states that the radius of curvature of the X-ray beam in the deformed regions of the crystal should exceed the *Pendellösung* distance (extinction length) by at least one order of magnitude. It is important to note that, for such deformations, interbranch scattering occurs only within a small part of the crystal, near the point z_0 where the Bragg condition is locally satisfied. We will consider a thin crystal whose thickness is appreciably less than the extinction length ξ_g. Still, the formalism covers crystal thickness from nanometre to micrometre values. This corresponds to the mesoscopic range, which plays an important role in semiconductors and metal compounds. Such structures may exhibit strong deviations from perfect periodicity, leading to values for the strain that render the eikonal approach inappropriate (Ibach, 1997; Kolosov & Tholen, 2000; Kim *et al.*, 2008).

It is worth pointing out that we develop a *microscopic* approach by rigorously summing the phases of the waves scattered by the misoriented domains. This may have advantages over the *macroscopic* (or phenomenological) approach, which operates with statistical parameters averaged over a volume of the reflection domain (Krivoglaz, 1996). The present approach will be especially important for high-quality crystals of small structures where statistical methods cannot be applied, owing to a small number of defects. The exact calculation of the phase changes allows the prediction of the phase modulation of the waves constituting the wavefield in deformed crystals. Phase modulation is caused by interbranch scattering, whereas amplitude modulation is induced by into-a-branch scattering.

2. Basic considerations

Assuming symmetrical X-ray Laue diffraction from a crystal with a one-dimensional deformation, which depends on the

Table 1
Table of the symbols introduced in the text.

Symbol	Expression	Explanation
z		Depth inside the crystal
z_0		Point where the Bragg condition is locally satisfied, such that $q(z_0) = 0$
$\mathbf{g}$		Diffraction vector
s		Departure of the incident wave from Bragg's law
$\mathbf{u}(z)$		Displacement field
ξ_g		X-ray extinction length for an ideal crystal
ω	$s\xi_g/(2\pi)$	Dimensionless departure
$D_{0,g}(z)$		Amplitudes of the transmitted and diffracted waves
$q(z)$	$[s + \mathbf{g}\,\mathrm{d}\mathbf{u}(z)/\mathrm{d}z]/2$	Deviation from Bragg's resonance in deformed crystal
$\eta(z)$	$[s + \mathbf{g}\,\mathrm{d}\mathbf{u}(z)/\mathrm{d}z]\xi_g/(2\pi)$	Dimensionless departure
$p(z)$	$\left(1 + \left\{[s + \mathbf{g}\,\mathrm{d}\mathbf{u}(z)/\mathrm{d}z]\xi_g/(2\pi)\right\}^2\right)^{1/2}$	Double value determines the splitting of the local dispersion surface in the conventional dynamical theory
$\Lambda(z)$	$4\pi^2\left\{1 + \left[q(z)\xi_g/\pi\right]^2\right\}/\left[\xi_g\mathbf{g}\,\mathrm{d}^2\mathbf{u}(z)/\mathrm{d}z^2\right]$	Inverse value determines the interbranch contribution to phase of the X-ray wavefield at the point z
$W(z)$	$(\pi/\xi_g)\left(1 + \left\{[s + \mathbf{g}\,\mathrm{d}\mathbf{u}(z)/\mathrm{d}z]\left(\xi_g/2\pi\right)\right\}^2\right)^{1/2}$	Phase deviation from interbranch contribution at the point z
$Q(z)$	$\left\{W^2(z) + [\pi/\Lambda(z)]^2\right\}^{1/2}$	Double value determines the interbranch splitting of the dispersion branches at the point z
Λ_g	$4\pi^2/\left[\xi_g\,\mathbf{g}\mathbf{u}''(z_0)\right]$	X-ray interbranch extinction length
ε	$\mathbf{g}\mathbf{u}''(0)\,\xi_g^2/(2\pi^2)$	Deformation parameter
$A^j_{0,g}(z)$		Modulation amplitudes
$\Phi^j_{0,g}(z)$	$[p(z)]^{-1/2}\exp\left[i\int S^j_{0,g}(z)\,\mathrm{d}z\right]$	Eikonal solutions of Takagi equation, related to the appropriate eikonal phase functions $S^j_{0,g}$
$C^{\pm}(z)$		Amplitudes of the upper and lower 'new' Bloch waves
$\psi(z)$	$-sz/2 + (zgu'/2 - gu)$	Phase term which does not depend on the interbranch contribution

depth in the crystal, Takagi's equations can be written as follows,

$$\frac{\mathrm{d}D_0(z)}{\mathrm{d}z} = \frac{i\pi}{\xi_g}D_g(z), \tag{1}$$

$$\frac{\mathrm{d}D_g(z)}{\mathrm{d}z} = \frac{i\pi}{\xi_g}D_0(z) + i\left[s + \mathbf{g}\,\frac{\mathrm{d}\mathbf{u}(z)}{\mathrm{d}z}\right]D_g(z), \tag{2}$$

where $D_{0,g}(z)$, $\mathbf{u}(z)$ and s are the amplitudes of the transmitted and diffracted waves, a long-range strain field and the departure of the incident wave from Bragg's law, respectively (see Table 1 for an explanation of the symbols used in the text). By differentiating (2) and using (1), one obtains the following equation for the amplitude $D_g(z)$,

$$\frac{\mathrm{d}^2D_g(z)}{\mathrm{d}z^2} - i\left[s + \mathbf{g}\,\frac{\mathrm{d}\mathbf{u}(z)}{\mathrm{d}z}\right]\frac{\mathrm{d}D_g(z)}{\mathrm{d}z} + \left[\left(\frac{\pi}{\xi_g}\right)^2 - i\mathbf{g}\,\frac{\mathrm{d}^2\mathbf{u}(z)}{\mathrm{d}z^2}\right]D_g(z) = 0. \tag{3}$$

The analytical solution of (3) is possible only for some special models of lattice displacements, one of which is the constant strain gradient model. Applying the method of Riemann and Laplace transforms, the appropriate rigorous solution expressed in terms of the confluent hypergeometric function was obtained by Litzman & Janacek (1974), Chukhovskii (1974) and Katagawa & Kato (1974). For simplicity, we assume that the displacement field $\mathbf{u}(z)$ is parallel to the surface. Thus the vector notation is hereafter omitted. In the case of homogeneous bending, its value has the form $u(z) = \alpha z^2/(2R)$, where R ($R > 0$) and α are the radius of curvature and a constant specifying the deformation, respectively. For a highly bent crystal, the confluent hypergeometric function yields the following asymptotic expression for the amplitude of the diffracted wave, which corresponds to the limit $R \to 0$ (Chukhovskii, 1980),

$$D_g(z) = \frac{i\pi}{\xi_g}\exp\left[2i\int_0^z q(z_1)\,\mathrm{d}z_1\right]\int_0^z \exp\left[-2i\int_0^{z_1} q(\zeta)\,\mathrm{d}\zeta\right]\mathrm{d}z_1. \tag{4}$$

Here, $q(z) = [s + g\,\mathrm{d}u(z)/\mathrm{d}z]/2$ and the amplitude of the incident wave is assumed to equal 1. However, this solution does not cover the whole range of the z values. It turns out that the asymptotic expression (4) cannot be applied within a small vicinity Δz_0 about the depth z_0 defined by $q(z_0) = 0$. Some simple considerations may be applied to verify this fact and assess the size of this vicinity. In this connection, one can deduce from (3) that the solution [equation (4)] is correct within a small fraction of $1/\varepsilon$, where $\varepsilon = \alpha g\xi_g^{\,2}/(2\pi^2R)$ and parameter $\varepsilon \gg 1$ for large gradient. On the other hand, as appears from (4), the changes of the amplitude $D_g(z)$ near the point z_0 achieve a value of the order of $1/\varepsilon$ within the small vicinity $\Delta z_0 = |z - z_0| \simeq \xi_g/\varepsilon$. Indeed, assuming for definiteness that $0 < z - z_0 \lesssim \xi_g/\varepsilon$, we portion all intervals of the integration in (4) into the interval from 0 to z_0 and the small interval from z_0 to $z - z_0$. After integrating, the amplitude $D_g(z)$ can be written as the sum of the value $D_g(z_0)$ and the small value proportional to $z - z_0$. It follows from this that the difference $\Delta D_g = |D_g(z_1) - D_g(z_2)|$, where the points z_1 and z_2 belong to the interval Δz_0, is less than or of the order of $1/\varepsilon$. Thus, within Δz_0 the changes in the magnitude of the amplitude $D_g(z)$, calculated from (4), are less than or of the order of $1/\varepsilon$ too. This is not in accordance with the accuracy of the asymptotic expression which is of the same order. Thus expression (4) incorrectly describes the wave amplitude within Δz_0. However, outside this vicinity the expression adequately describes X-ray diffraction in a strongly deformed crystal (Shevchenko, 2007). Moreover, as it appears from the presented arguments, expression (4) can be applied for an arbitrary model of one-dimensional deformation, such that it can be considered as asymptotic of the rigorous solution, when passing to the limit of large gradient. Therefore, the discussion following (4) may be put forward irrespective of the choice of mathematical model for the strain field.

Clearly, this problem with the asymptotic solution [equation (4)] is as expected, because this expression only describes the X-ray kinematical diffraction in a strongly deformed crystal. At the same time, near the point z_0 the dynamical interbranch processes are resonantly activated with increasing deformation. It should be noted that calculation of the interbranch contribution with the help of Takagi equations may run into serious difficulties. The point is that these equations describe both interbranch and into-a-branch scattering which, in the kinematical diffraction limit, determine the maximum of the X-ray rocking curve. Thus it is convenient to apply the 'eikonal' representation of the dynamical theory. Within this representation the into-a-branch contribution is extracted from the X-ray wavefields, by expanding the amplitudes D_0 and D_g in a series of eikonal basic functions. These functions are related to the modified Bloch waves introduced by Kato (1963, 1964). The expansions for the amplitudes take the form

$$D_{0,g}(z) = \exp\left[i\int_0^z q(z_1)\,\mathrm{d}z_1\right]\sum_{j=1,2} A^j_{0,g}(z)\Phi^j_{0,g}(z), \qquad (5)$$

where $\Phi^{1,2}_{0,g}(z)$ are the eikonal solutions for the transmitted and diffracted waves of Takagi's equations for the 'upper' and 'lower' dispersion branches, respectively; $A^j_{0,g}(z)$ are the modulation amplitudes which correspond to the appropriate eikonal solutions. In the case of a one-dimensional deformation with variable strain gradient considered hereafter, the basic function can be taken from (Shevchenko, 2005)

$$\Phi^j_{0,g}(z) = \frac{1}{[p(z)]^{1/2}}\exp\left[i\int S^j_{0,g}(z)\,\mathrm{d}z\right],$$

where the eikonal phase functions are

$$S^j_{0,g}(z) = \frac{\pi}{\xi_g}p(z) + i\frac{\eta'(z)}{2p(z)} \quad \text{and} \quad S^1_{0,g}(z) = -S^2_{0,g}(z).$$

Here $p(z) = [1+\eta^2(z)]^{1/2}$, the deviation $\eta(z) = \omega + g(\mathrm{d}u/\mathrm{d}z)\xi_g/(2\pi)$ and the departure $\omega = s\xi_g/(2\pi)$. Of special interest among the 'new' waves are those propagating in the transmitted channel, in which the interbranch scattering can induce a 'jump' of the tie point. In this connection, we will consider the fundamental equations for the amplitudes $A^{1,2}_{0,g}(z)$ only, which can be obtained by substituting (5) into Takagi's equations,

$$\frac{\mathrm{d}A^{1,2}_0(z)}{\mathrm{d}z} = -\frac{A^{2,1}_0(z)\exp\left[\mp(2i\pi/\xi_g)\int_0^z p(z_1)\,\mathrm{d}z_1\right]}{2p^2(z)\left[\omega \pm (1+\omega^2)^{1/2}\right]}\frac{\mathrm{d}\eta(z)}{\mathrm{d}z}. \qquad (6)$$

In analogy with the study of the interbranch interchange carried out for homogeneous bending by Shevchenko (2003), we introduce the interbranch extinction length $\Lambda_g = 2\pi p^2(z_0)/\eta'(z_0)$. It should be noted that for a uniform strain gradient the interbranch extinction length determines the effective period of the oscillations of the diffracted wave, which are due to the X-ray interbranch scattering (Shevchenko, 2007). Besides, the inverse value $k_\Lambda = 1/\Lambda_g$ specifies the increment of the amplitudes of the 'new' waves per unit length. For weak deformation, the value $k_\Lambda \ll 1/\xi_g$ and, as it appears from (6), the derivatives $\mathrm{d}A^{1,2}_0(z)/\mathrm{d}z$ tend to zero. This means that the appropriate amplitudes $A^{1,2}_0(z)$ are the constants corresponding to the eikonal approximation of the dynamical diffraction theory. However, when a crystal is strongly deformed, $k_\Lambda \gg 1/\xi_g$. In this case the interbranch contribution is rapidly accumulated, leading to sharp changes of the modulation amplitudes near z_0. The large value of k_Λ is also associated with the anomalous splitting of the dispersion branches. Using the considerations given by Shevchenko (2005), one can deduce that the interbranch splitting at the point z is described by the value $2Q(z) = 2\{W^2(z) + [\pi/\Lambda(z)]^2\}^{1/2}$, where $W(z) = \pi p(z)/\xi_g$ and $\Lambda(z) = 2\pi p^2(z)/\eta'(z)$ such that $\Lambda(z_0) = \Lambda_g$. Taking into account rigorously the interbranch changes of the phases of the 'new' waves, the amplitude of the transmitted wave can be written as

$$D_0(z) = \exp\left[i\int_0^z q(z_1)\,\mathrm{d}z_1\right]\left\{C^+(z)\exp\left[i\int_0^z Q(z_1)\,\mathrm{d}z_1\right] + C^-(z)\exp\left[-i\int_0^z Q(z_1)\,\mathrm{d}z_1\right]\right\}, \qquad (7)$$

where $C^\pm(z)$ is the amplitude of the 'new' Bloch wave corresponding to the 'new' Bloch wavevector $\pm Q(z)$. Owing to the interbranch jump of the 'tie point', the energy of X-rays will be transferred from the 'new' upper Bloch wave to the 'new' lower one. This leads to a change of the amplitude $C^+(z)$ from 1 to 0 within the small vicinity Δz_0, while the amplitude $C^-(z)$ changes from 0 to 1. (Any attenuation of the incident wave through the crystal by diffraction is neglected.) Clearly, these changes have to occur within the small vicinity of z_0. Therefore, we will approximate them by step functions, by supposing that $C^+(z) = \Theta^+(z_0 - z)$ and $C^-(z) = \Theta^-(z_0 - z)$, where $\Theta^+(z)$ equals 1 and 0 if $z > 0$ and $z < 0$, respectively, whereas $\Theta^-(z)$ equals 1 and 0 if $z < 0$ and $z > 0$, respectively. It should be noted that this approximation is not critical for the final conclusions. The point is that they are mainly based on the concept of the interbranch changes of the phase of the X-ray wavefields, which does not depend on the given assumption. As a result, (7) can be modified to

$$D_0(z) = \exp\left\{ i \int_0^z \left[q(z_1) + \Theta(z_0 - z) Q(z_1) \right] \mathrm{d}z_1 \right\}, \qquad (8)$$

where $\Theta(z)$ equals 1 and -1 if $z > 0$ and $z < 0$, respectively. For calculation of the amplitude D_g, which contains the interbranch contribution to the phase of the transmitted wave, we use the integral form of (2), which is the exact relation among the amplitudes D_g and D_0. Then, it is straightforward to obtain the following expression for the amplitude of the diffracted wave,

$$D_g(z) = \frac{i\pi}{\xi_g} \exp\left[2i \int_0^z q(z_1)\,\mathrm{d}z_1 \right] \times \int_0^z \exp\left\{ i \int_0^{z_1} \left[-q(z_2) + \Theta(z_0 - z) Q(z_2) \right] \mathrm{d}z_2 \right\} \mathrm{d}z_1. \qquad (9)$$

As one can see, we extend the expression for $D_g(z)$, obtained previously for a homogeneously bent crystal (Shevchenko, 2007), to the case of any form of continuous one-dimensional deformation. This result is not accidental and is due to the covariant form of the fundamental equations corresponding to the 'eikonal' representation of the X-ray dynamical theory used to obtain the diffracted intensity. It is obvious that these equations depending on the parameters $p(z)$, $\eta(z)$, ω and ε have an identical form for different models of the variations of lattice distortions with the depth z inside the crystal. Therefore, the form of the expression for the diffracted intensity for variable strain gradients is the same as that corresponding to a constant strain gradient.

In contrast to the kinematical relation [equation (4)], the dynamical interbranch contribution is taken into account in this expression. Furthermore, analyzing (9), it is interesting to note that only the correct phase relation in (8), involving considerations of the interbranch scattering, allows the X-ray kinematical diffraction limit in a highly deformed crystal to be obtained. Indeed, in (9), it is possible to replace the value $Q(z)$ by the value $|q(z)|$ at any point z which is far from z_0. Then (9) transforms into the appropriate expression for the kinematical amplitude of the diffracted wave, which is analogous to (4).

After a straightforward manipulation (see Appendix *A*), (9) can be reduced to the form

$$D_g(z) = \frac{i\pi}{\xi_g} \exp\left[2i \int_0^z q(z_1)\,\mathrm{d}z_1 \right] \times \int_0^z \exp\left\{ i \left[\psi(z_1) + \Theta(z_0 - z) Q(z_1) z_1 \right] \right\} \mathrm{d}z_1, \qquad (10)$$

where $\psi(z) = -sz/2 + (zgu'/2 - gu)$. As it appears from (10), the interbranch scattering causes the phase modulation of the X-ray diffracted wave near the point z_0. Obviously, the effective period of the modulation will be of the order of the X-ray interbranch extinction length Λ_g. As $\Lambda_g \ll \xi_g$, the effect of the phase modulation may be very pronounced for a thin crystal, whose thickness t is considerably less than the conventional extinction length ξ_g. Bearing in mind the order of magnitudes possible for ξ_g, one can estimate that the appropriate thickness t may vary from nano-scaled values to micro-sized ones. The latter case corresponds to a crystal with sufficiently large ξ_g (as, for example, protein crystals). At the same time, this range is the threshold for the advanced technical applications directed at fabrication of small-sized devices. Therefore, this study of the X-ray interbranch processes in a highly deformed crystal has a practical application too. Generally, the presented theory allows the description of the X-ray diffraction within a small spatial range which is not covered by the asymptotic behavior of the rigorous solution.

3. X-ray diffracted intensity from a crystal with an exponential strain gradient

The phase modulation of the diffracted wave owing to interbranch scattering may lead to prominent features in the diffracted intensity function. These features directly follow from (10), which we will apply to a model involving an exponential strain gradient. Thus, it will be assumed that the displacement field has the form $u(z) = u_0 \exp(-z/l)$, where u_0 and l are the amplitude of the deformation and the characteristic depth of the changes of the deformation, respectively. Then, it follows from (10) that the X-ray diffracted intensity *versus* the deviation parameter ω is described by the expression

$$I_g(\omega) = \frac{1}{\varepsilon^2} \left| \int_0^\tau \exp\left\{ i \left[\psi_{\exp}(\zeta) + \Theta(\zeta_0 - \zeta) Q_{\exp}(\zeta) \zeta / \varepsilon \right] \right\} \mathrm{d}\zeta \right|^2, \qquad (11)$$

where the dimensionless variable $\zeta = \varepsilon\pi z/\xi_g$, such that $\tau = \varepsilon\pi t/\xi_g$, and, moreover, we denote

$$\psi_{\exp}(\zeta) = -\frac{\omega}{\varepsilon} z - \left(\frac{2\varepsilon}{a} + \zeta \right) \frac{\exp(-a\zeta/\varepsilon)}{a}, \qquad (12)$$

$$Q_{\exp}(\zeta) = \left\{ 1 + \eta^2(\zeta) + \frac{\varepsilon^2 \exp(-2a\zeta/\varepsilon)}{4[1 + \eta^2(\zeta)]^2} \right\}^{1/2}, \qquad (13)$$

where $\eta(\zeta) = \omega - (\varepsilon/a)\exp(-a\zeta/\varepsilon)$ and $a = \xi_g/(\pi l)$. In (11)–(13), we use the notation $\varepsilon = \eta'(0)\xi_g/\pi$ which is also valid for homogeneous bending. In the case of an exponential strain gradient, the deformation parameter $\varepsilon = gu_0\xi_g^2/(2\pi^2 l^2)$, such that the interbranch extinction length $\Lambda_g = 2\xi_g/\varepsilon$. It should also be noted that by introducing the variable ζ it becomes straightforward to calculate the diffracted intensity for strong deformation. At the same time, as it appears from (10), this expression can be extended to the case of a weak deformation too. Indeed, for a slightly deformed crystal, the parameter $\varepsilon \ll 1$. Therefore, the interbranch phase contribution in (10), which is proportional to ε, will be small for such distortions, producing a negligible effect on the diffracted intensity. Thus, (10) can be exploited for any strength of the deformation of a thin crystal. For this purpose we introduce the variable $\tilde{z} = z\pi/\xi_g$ for a weak distortion, while for a strong deformation we will use the variable ζ, expressed above. The results of the numerical calculations of the X-ray rocking curve for the different deformations are shown in Figs. 1, 2 and 3. They are obtained by applying the model parameters t = 300 nm, ξ_g = 10 µm, a = 10 and ε = 0.01, 10 and 100. (It should also be noted that in terms of the units of length Λ_g, the given thickness $t = 1.5\Lambda_g$ in the case of ε = 100.)

As one can see from Fig. 1, corresponding to a small distortion, the diffracted intensity has no remarkable features, owing to the small interbranch term. If deformation slightly exceeds the eikonal limit of the dynamical theory, a weakly prominent interbranch splitting appears in the X-ray rocking curve (see Fig. 2). In this case, the interbranch splitting occurs within the small angular range $\Delta\omega_{\rm int}$, which is appreciably less than the half-width of the X-ray rocking curve $\Delta\omega_{1/2}$.

With increasing deformations, the interbranch scattering increases too, such that the splitting effect will be the most prominent when $t \simeq \Lambda_g$. This is illustrated by Fig. 3, corresponding to the strong deformation ε = 100. It is worth pointing out that the interbranch splitting is the extinction feature of X-ray diffraction with a highly deformed crystal. In fact, the interbranch contribution to the phase of the transmitted wave can be considered as the effective deviation from Bragg's law, which leads to losses of the kinematical intensity. Moreover, owing to activation of the interbranch processes, the diffracted intensity as a function of depth in the crystal may show the prominent interbranch oscillations near the point satisfying the local Bragg conditions. This is demonstrated in Fig. 4, where the intensity is plotted as a function of the variable ζ, for the deformation ε = 100 and the value a = 10. It should be noted that the number of oscillations grows when the values of z and ω are increased.

When the crystal thickness is increased, the half-width $\Delta\omega_{1/2}$ of the rocking curve decreases. Therefore, interbranch scattering in a thick crystal will not split the top of the Bragg peak, but may cause an asymmetrical appearance of its shape. This is shown in Fig. 5. Actual values of the parameters are ε = 100, a = 10 and thickness t = 1.2 µm, corresponding to $6\Lambda_g$. As may be seen, for a sufficiently thick crystal the interbranch

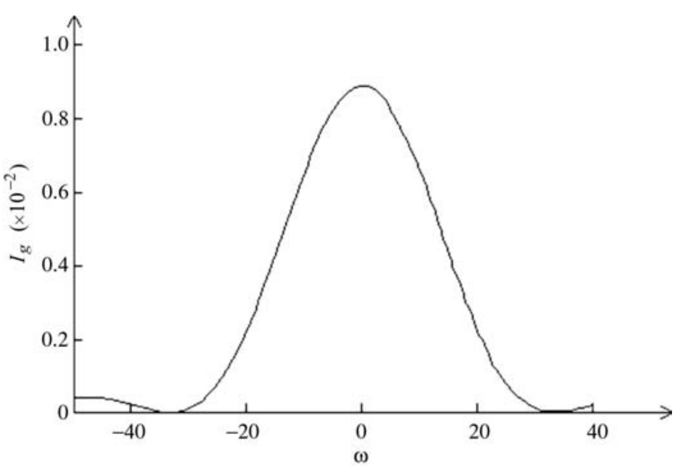

Figure 1
X-ray rocking curve for weak deformation ε = 0.01.

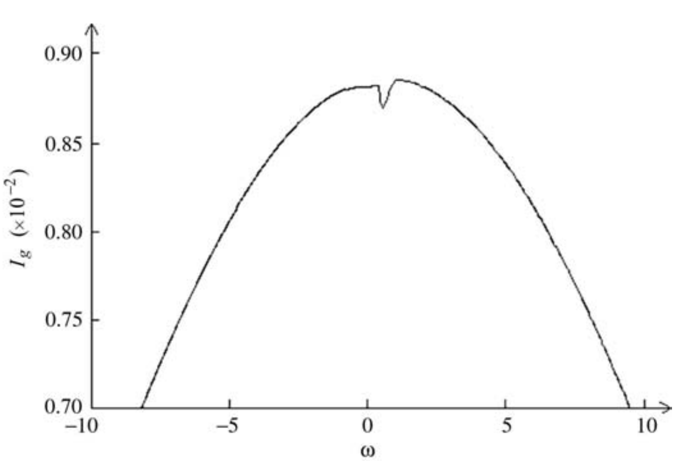

Figure 2
Interbranch splitting of the Bragg peak, which corresponds to ε = 10.

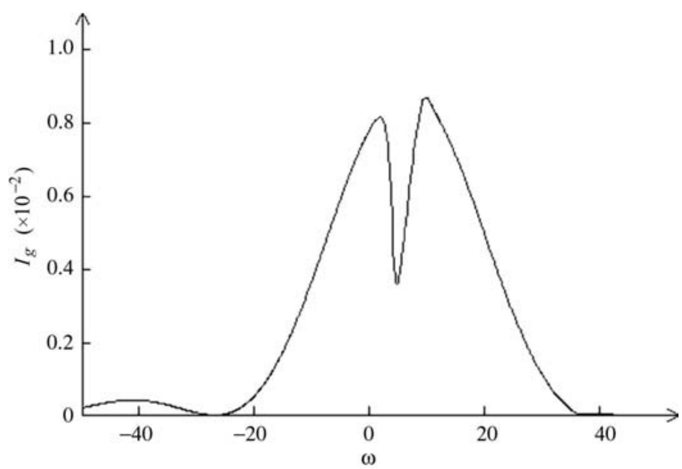

Figure 3
Interbranch splitting of the diffracted intensity from a highly deformed crystal, specified by ε = 100.

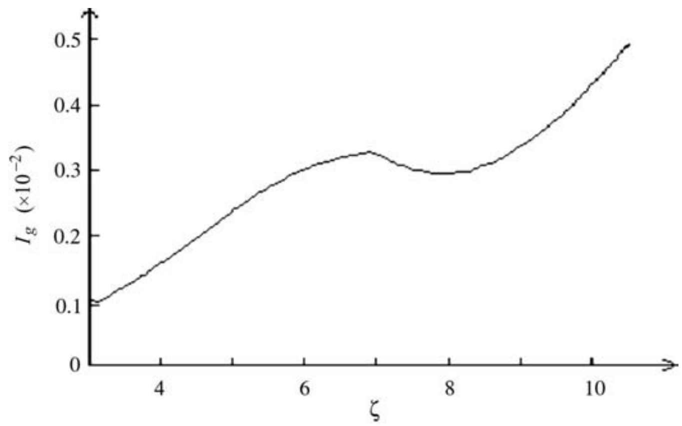

Figure 4
Interbranch variations of the diffracted intensity *versus* ζ, near the point ζ_0 = 6.9, related to the departure ω = 5.

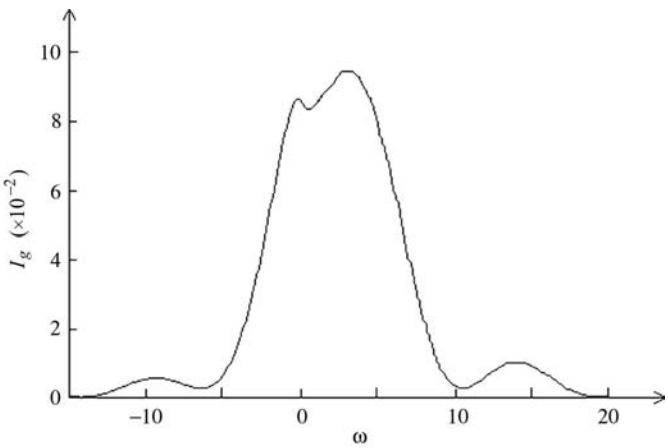

Figure 5
Asymmetrical broadening of the Bragg peak when the thickness t = 1.2 μm.

splitting is actually degenerated and the Bragg peak tends to be transformed into the asymmetrical form.

Analyzing the plotted curves, one can deduce that the X-ray rocking curves calculated for the exponential deformation are similar to the curves obtained for a homogeneously bent crystal (Shevchenko, 2007). In both cases the diffracted intensities reveal interbranch anomalies, which apparently occur for any form of continuous distortion. Characteristically, these features are very sensitive to small changes in the crystal thickness. Changes of a few hundred nanometres may considerably influence the shape of the X-ray rocking curve. In this connection, we suggest that study of the interbranch features occurring in the X-ray rocking curves may be of interest for an accurate determination of the thickness of a strongly deformed crystal within the submicrometre or even the nanometre length range.

4. Extinction contrast in the case of a highly distorted specimen

The interbranch scattering responsible for the prominent anomalies in the diffracted intensity may also lead to extinction features in the integrated diffracted intensity. This follows also from the presented numerical results for the exponential strain gradient, which show considerable interbranch losses of the diffracted intensity. Thus one may anticipate that the integrated diffracted intensity for a strongly deformed thin crystal will not vary linearly with thickness as follows from the conventional theory. One should pay attention to this fact in the study of extinction contrast from an isolated defect in a thin crystal. In this connection, it is necessary to remember that the conventional theory predicts the disappearance of the contrast if the crystal is sufficiently thin (Penning & Goemans, 1968; Tanner, 1972). On the other hand, as appears in the present approach, an image of a defect may arise in the case of a strongly deformed thin specimen. Bearing this in mind, we consider the image from a single dislocation which exhibits double contrast. The image width, D, of the double contrast, explained as a direct or kinematical image by Authier (1967), can be estimated as

$$D \simeq \xi_g. \tag{14}$$

The direct image originates from the deformed regions, positioned near the dislocation core, in which the absolute value of effective misorientation δ exceeds the perfect crystal reflection range $\Delta\psi_{1/2}$ associated with the X-ray dynamical diffraction. (For convenience of the further considerations, we introduce angular variables instead of dimensionless variables ω and $\Delta\omega_{1/2}$ used above.) However, these considerations are based on the supposition that the into-a-branch dynamical process producing the *Pendellösung* phenomenon mainly contributes to the diffracted intensity from the crystal matrix. At the same time, in the strongly distorted crystal, the dominant interbranch scattering, producing the phase modulation of the diffracted wave, leads to the reduction of the extinction length to the value $\Lambda_g = 2\xi_g/\varepsilon$ ($\varepsilon \gg 1$), which is called the interbranch extinction length. This means that for strong deformation the angular range $\Delta\psi_{\rm int}$ of the interbranch losses of the diffracted intensity will be of the order of the value $1/(g\Lambda_g) \simeq \varepsilon\Delta\psi_{1/2}$. Hence, the interbranch contribution to the diffracted intensity can be neglected for the misorientations δ around the dislocation core which exceed the value $\varepsilon\Delta\psi_{1/2}$. As a consequence, the estimation [equation (14)] for the image width should be rewritten for a highly distorted matrix as

$$\begin{aligned} D &\simeq 1/(g\Delta\psi_{\rm int}) \simeq \xi_g/\varepsilon, \\ D &\simeq \Lambda_g. \end{aligned} \tag{15}$$

As can be seen from (15), assuming strong deformation, the width of the dislocation image considerably decreases. Consequently, the image may only be visible for crystals having a large value of ξ_g. In this connection, one can predict that the extinction contrast will be most prominent for deformed protein crystals specified by values of ξ_g of the order of 10^3 μm.

It is interesting to note that the image width from a screw dislocation in a protein crystal has been analyzed by Koizumi *et al.* (2005). It was found that the calculated value D, which is of the order of 10^3 μm using (14), is greater than the measured value by two orders of magnitude. Furthermore, the theoretical rocking curve width, which is of the order of 10^{-5} deg, turned out to be less than the measured $\Delta\psi_{1/2}$ by two orders of magnitude. The authors explained these effects by the high mosaicity of the protein crystal. On the other hand, the appreciable increase of the half-width $\Delta\psi_{1/2}$ implies a very small average size of the mosaic blocks compared with the extinction length ξ_g. Along with this, for visibility of the image, the conventional theory dictates the minimal conditions $0.4\xi_g$ in the crystal thickness, which was verified for a protein crystal (Tachibana *et al.*, 2003). However, supposing a strong deformation of the matrix around the dislocation, we can verify the reported suggestion. Indeed, according to the considerations given above, extinction contrast may be formed even in the case of a thin deformed matrix, where its thickness satisfies $\Lambda_g \lesssim t \ll \xi_g$. Then, we will suggest that the dislocation core is contained in the strongly deformed block specified by the deformation $\varepsilon \simeq 10^2$, related to the value $\Lambda_g \simeq 10$ μm which will also determine the thickness of the mosaic blocks. Taking this into account, we obtain estimations for the values D and $\Delta\psi_{1/2}$ which coincide with the experimental results.

The given example shows that study of the interbranch scattering in a strongly deformed specimen might be useful for the structure determination of an organic crystal and, moreover, it would help to improve the understanding of the formation of a dislocation image in crystals having a large value of ε.

5. Conclusions

Here we sum up the main results obtained in this work.

In the case of a sharp strain gradient, the interbranch processes are analyzed in a one-dimensional deformed crystal. It is shown that a combination of Takagi's equations with the fundamental equations corresponding to the 'eikonal' representation allows the interbranch contribution to the phase of the X-ray wavefield to be rigorously calculated. At the same time, the conventional approach based on Takagi's equations solely leads to the kinematical expression for the diffracted amplitude, which is not applicable near the point z_0.

For an exponential strain gradient, the diffracted intensity is calculated for different strengths of deformation in a thin crystal. It is established that, with increasing deformation, observable extinction features, owing to the interbranch phase modulation, arise in the X-ray rocking curve. This requires that the thickness of the crystal, t, is of the same order of magnitude as the interbranch extinction length Λ_g. The value Λ_g depends on the deformation and the conventional extinction length ξ_g, such that it may be changed from the nanoscaled to mesoscopic ranges.

The extinction contrast from an isolated defect is also considered for a strongly deformed crystal specified by a large value of the parameter ε. It is deduced that, owing to the interbranch scattering in the deformed matrix, the extinction contrast may appear even in the case of a very thin specimen, whose thickness t is appreciably less than ξ_g. It is estimated that the appropriate width of the dislocation image will be of the order of the interbranch extinction length Λ_g. This result is in line with the available experimental data obtained for a screw dislocation in a protein crystal.

APPENDIX *A*
Calculation of the phase integrals

Let us carry out the mathematical manipulations with the integral

$$I(z) = \int\limits_0^z \exp\left[-i\int\limits_0^{z_1} q(z_2)\,\mathrm{d}z_2 + i\Theta(z_0 - z)\int\limits_0^{z_1} Q(z_2)\,\mathrm{d}z_2\right]\mathrm{d}z_1. \tag{16}$$

By integrating the second phase integral in (16) by parts, we modify it to the expression $Q(z)z - \int_0^z Q'(z_1)z_1\,\mathrm{d}z_1$. As to the latter integral, it can be written as

$$\int\limits_0^z Q'(z_1)z_1\,\mathrm{d}z_1 = \left(\frac{\pi}{\xi_g}\right)^2 \int\limits_0^z p(z_1)p'(z_1)\frac{\mathrm{d}z_1}{Q(z_1)} + \frac{1}{4}\int\limits_0^z \frac{\eta'(z_1)\eta''(z_1)}{Q(z_1)p^4(z_1)} z_1\,\mathrm{d}z_1. \tag{17}$$

In (17), we neglect any small terms and will denote the second integral by $I_0(z)$. It should be noted that the integral $I_0(z)$ is attributed only to deformation with variable strain gradient. Therefore we pay special attention to calculation of this integral. In this connection, we take into account the relation $\eta'(z) \gg \pi/\xi_g$, which implies that the integrand in $I_0(z)$ is appreciable only near z_0. In the result, it can be replaced by the expression $(1/2)\eta''(z)z/p^2(z)$. Moreover, we will assume that the strain field has the form $u(z) = u_0 f(z)$, where u_0 is the amplitude of the deformation and, for definiteness, it is also assumed that $f(0) = 1$. Bearing this in mind, we assess the value $\eta''(z)$ as $\varepsilon\pi f(z)/(l\xi_g)$, where $\varepsilon = gu_0\xi_g^2/(2\pi^2 l^2)$ and l is the characteristic range of the changes of the displacement field. Then suggesting $\eta(z) \simeq \eta'(z_0)(z - z_0)$ and taking $\eta'(z_0) \simeq \varepsilon\pi f(z_0)/\xi_g$, one can obtain

$$I_0 \simeq \frac{\xi_g}{2\pi l}\int\limits_0^\zeta \frac{\Delta}{\Delta^2 + (\zeta - \zeta_0)^2}\frac{f(\zeta_1)}{f(\zeta_0)}\zeta_1\,\mathrm{d}\zeta_1, \tag{18}$$

where $\zeta = \varepsilon\pi z/\xi_g$ and $\Delta = 1/[\varepsilon f(\zeta_0)]$. Because for strong deformations $\Delta \ll 1$, the first multiplier in the integrand in (18) can be considered as the delta function. Thus, the integral $I_0 \simeq z_0/(2l)$. This value does not depend on z. Hence, the second term in (17) will not contribute to the diffracted intensity and can be omitted. At the same time, the first integral in (17) is significant only far from z_0, where $Q(z) \simeq |q(z)|$. Taking this into account, one may deduce that this term is $\Theta(z_0 - z)(gu - zgu')/2$. It follows from this, after a straightforward manipulation, that the integral $I(z)$ equals $\int_0^z \exp\{i[\psi(z_1) + \Theta(z_0 - z)Q(z_1)z_1]\}\,\mathrm{d}z_1$, where the phase $\psi(z) = -sz/2 + (zgu'/2 - gu)$.

The author wishes to thank Emeritus Professor Andre Authier, who gave many suggestions and insights when reviewing the manuscript.

References

Authier, A. (1967). *Adv. X-ray Anal.* **10**, 9–31.
Authier, A. (2005). *Dynamical Theory of X-ray Diffraction.* Oxford University Press.
Authier, A. & Balibar, F. (1970). *Acta Cryst.* A**26**, 647–654.
Chukhovskii, F. (1974). *Kristallografiya*, **19**, 482–488.
Chukhovskii, F. (1980). *Metallofizica*, **2**, 3–27.
Ferrari, C., Armani, N. & Verdi, N. (2005). *J. Phys. D*, **38**, A143–A146.
Ibach, H. (1997). *Surf. Sci. Rep.* **29**, 193–263.
James, R. (1948). *The Optical Principles of the Diffraction of X-rays.* London: G. Bell and Sons.
Katagawa, T. & Kato, N. (1974). *Acta Cryst.* A**30**, 830–836.
Kato, N. (1963). *J. Phys. Soc. Jpn*, **18**, 1785–1791.
Kato, N. (1964). *J. Phys. Soc. Jpn*, **19**, 67–77.
Kim, D., Jong, J., Kim, H., Cho, K. & Kim, S. (2008). *Thin Solid Films.* **516**, 7715–7719.

Koizumi, H., Tachibana, M., Yoshizaki, I. & Kojima, K. (2005). *Philos. Mag.* **85**, 3709–3713.
Kolosov, V. & Tholen, A. (2000). *Acta Mater.* **48**, 1829–1840.
Krivoglaz, M. (1996). *X-ray and Neutron Diffraction in Nonideal Crystals.* Berlin: Springer Verlag.
Litzman, O. & Janacek, Z. (1974). *Phys. Status Solidi A*, **25**, 663–666.
Penning, P. (1966). PhD Thesis, Technical University of Delft, The Netherlands.
Penning, P. & Goemans, A. (1968). *Philos. Mag.* **18**, 297–300.
Shevchenko, M. (2003). *Acta Cryst.* A**59**, 481–486.
Shevchenko, M. (2005). *Acta Cryst.* A**61**, 512–515.
Shevchenko, M. (2007). *Acta Cryst.* A**63**, 273–277.
Tachibana, M., Koizumi, H., Izumi, K., Kajiwara, K. & Kojima, K. (2003). *J. Synchrotron Rad.* **10**, 416–420.
Takagi, S. (1969). *J. Phys. Soc. Jpn*, **26**, 1239–1253.
Tanner, B. (1972). *Phys. Status Solidi A*, **10**, 381–386.
Tanner, B. K. & Hill, M. (1986). *Adv. X-ray Anal.* **29**, 337–343.